Metrol. Meas. Syst., Vol. 29 (2022) No. 3, pp. 553–571
DOI: 10.24425/mms.2022.142269

PAN POLSKA AKADEMIA NAUK

METROLOGY AND MEASUREMENT SYSTEMS
Index 330930, ISSN 0860-8229
www.metrology.wat.edu.pl

M&MS

ANALYSIS AND APPLICATION OF REAL-TIME COMPENSATION OF POSITIONING PRECISION OF THE TURNTABLE WITH A HARMONIC FUNCTION

Yi Zhou[1)], Weibin Zhu[1)], Yi Shu[1)], Yao Huang[2,3)], Wei Zou[3)], Zi Xue[3)]

1) *China Jiliang University, School of Measurement and Testing Engineering, Hangzhou, 310018, China* (✉ *zhuweibin@cjlu.edu.cn*, +86 13 588 068 692)
2) *Zhejiang University, College of Optical Science and Engineering, State Key Laboratory of Modern Optical Instrumentation, Hangzhou 310027, China* (*huangyao@nim.ac.cn*)
3) *National Institute of Metrology, Beijing, 100029, China* (*huangyao@nim.ac.cn*)

Abstract

In order to guarantee the accuracy of turntable angle measurement, a real-time compensation method for turntable positioning precision based on harmonic analysis is proposed in this paper. Firstly, the principle and feasibility of the real-time compensation method are analysed, and a detailed description of harmonic compensation is provided herein. Secondly, we analyse the relationships between the surface number of the polygon with the compensation order of the harmonic function and its corresponding compensation accuracy. The effects of the iterations number and the data width on calculation accuracy in the coordinate rotation digital computer (CORDIC) algorithm are analysed and the quantization models of the approximation error and rounding error of the CORDIC algorithm are established. Then, the calculation of the harmonic error function and real-time compensation processes are implemented on a field programmable gate array (FPGA) chip. The resource occupation and time delay of the phase angle calculation and the harmonic component calculation are discussed separately. Finally, the validity of the harmonic compensation method is proven through comparing the compensation effect with that of linear interpolation and the polynomial compensation method. The influences of the compensation order, the iterations number and the data width on the compensation results are demonstrated by simulation. A test platform with a laboratory-made FPGA circuit is built to evaluate the effect of real-time compensation with the harmonic function and the positioning error compensation can be performed within 760 ns. The results confirmed the effectiveness of the harmonic compensation method, revealing an improvement of the positioning precision from 54.21″ to 1.63″, equivalent to 96.99% reduction in positioning error.

Keywords: harmonic function, positioning error, compensation, real-time, CORDIC.

1. Introduction

The turntable is an important device in high precision measurement and metrology, and as suchit is widely used in aeronautics, industrial and medical treatment [1]. The positioning

Article history: received February 10, 2022; revised April 26, 2022; accepted June 8, 2022; available online July 28, 2022.

precision of the turntable is influenced by the error of posture, component size and so on. Therefore, it is essential to improve the positioning precision by means of compensation methods so as to meet the high accuracy requirements of angle measurement.

The positioning precision compensation methods can be divided into two kinds: hardware compensation and software compensation. Hardware compensation can be generalized as increasing the number of reading heads. In 1998, Probst [2] proposed a method which used 16 non-uniformly distributed reading heads and reduced the uncertainty of measurement to less than $0.01''$ ($k = 2$). In 2001 and 2003, the Equal-Division-Averaged method was presented by Watanabe [3, 4] and 5 reading heads were used to reduce the uncertainty of measurement to $\pm 0.02''$. In 2014, Watanabe [5] proposed a method which he used 8 non-uniformly distributed reading heads, and the accuracy of $\pm 0.03''$ at any given angle was achieved. In 2018, Huang [6] established the EDA model which used 4 reading heads, and the uncertainty of measurement was $\pm 0.05''$ ($k = 2$). Although high positioning precision can be achieved by increasing the number of reading heads s or changing the layout position, the cost and complexity of an angle measuring system also increases accordingly. In addition, the number of reading heads that can be arranged on a turntable is also limited.

Comparing with hardware compensation, software compensation [7] has numerous advantages, such as lower cost, greater flexibility and higher positioning precision. Therefore, the software compensation method has gradually become the research focus in recent years. In 2009, Dhar [8] proposed a neural network-based error compensation method, and the turntable's positioning error was reduced down to ±6 arcmin. In 2011, a compensation method based on nonlinear least squares was presented by Guanbin [9], and the positioning error was decreased from 0.008° to $28.8''$ by calculating eccentric parameters. In 2012, Lopez [10] used lookup tables that were built by linear interpolation and Lissajous plot to compensate the turntable positioning errors. The *Single Gimbals Control Moment Gyroscope* (SGCMG) compensation method, which can reduce the systematic cost and positioning error of a circular grating, was proposed by Yu [11] in 2020. Jia [12] proposed a method based on the Fourier *expansion-back propagation* (BP) neural network optimized by a genetic algorithm in 2020, and the measurement error was decreased from $110.2''$ to $2.7''$. In 2021, Du [13] reduced the positioning error of a single reading head by 93.76% with the first and second harmonic fitting method. In 2021, Gurauskis [14] disclosed a technique which used polynomial fitting to compensate the encoder's positioning error and reduced the error by 98%.

However, each of these methods, as well as other related ones that have not been listed here, has one general characteristic in i.e. the positioning error compensation process is realized in the off-line mode with a computer.

In this study we proposed a real-time compensation method that used harmonic analysis. On the basis of the description of the feasibility of the real-time compensation method and the principle of harmonic compensation analysis, we discussed the relationship between the surface number of the polygon with the order of the harmonic function and its corresponding compensation accuracy. Quantization models of the approximation error and the rounding error were built by analysing the data width and the iterations number of the *coordinate rotation digital computer* (CORDIC) algorithm. A laboratory-made circuit board using a *field programmable gate array* (FPGA) was developed to realize the real-time compensation process and the system performance and resource occupation were analysed. The feasibility of the real-time compensation method was proved through conducting experiments, and the quantitative models of key parameters were verified with the circuit. We also discuss the effectiveness of the method and report the effects of the real-time compensation with the harmonic function.

Metrol. Meas. Syst., Vol. 29 (2022), No. 3, pp. 553–571
DOI: 10.24425/mms.2022.142269

2. Principle of real-time harmonic compensation method

2.1. Principle of the real-time compensation method

In practice, the real-time compensation method is realized in two steps of the positioning error function acquisition and the positioning error compensation. The positioning error function is obtained through calibration, which is based on the circumferential closure of the turntable. The characteristic of periodicity and repetitiveness of the turntable positioning error is the basis to complete real-time compensation through a hardware platform. The schematic of a typical real-time compensation process is shown as Fig. 1.

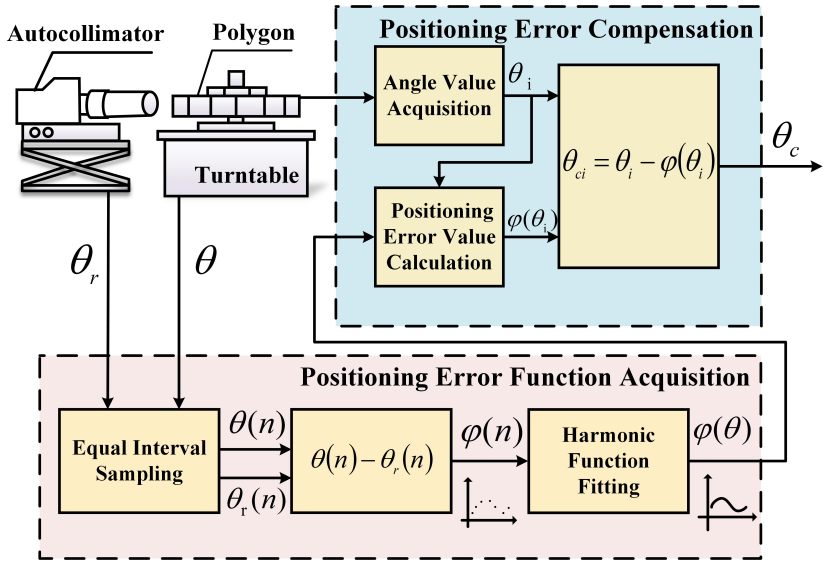

Fig. 1. Schematic representation of real-time compensation for positioning error.

As shown in Fig. 1, in the first part of the positioning error function acquisition, we use the autocollimator and the polygon to implement positioning calibration of the turntable. Due to the periodicity of the rotating angle, we can calibrate the reference values around a circle with equal angle-intervals. The values are defined as $\theta(n)$ $(n = 1 \ldots N)$, where N is the surface number of polygon. Meanwhile, the discrete angle values at the calibrated positions are recorded, defined as $\theta_r(n)$ $(n = 0 \ldots N)$. So, the corresponding positioning error sequence of the turntable, defined as $\varphi(n)$ $(n = 0 \ldots N)$, can be described as:

$$\varphi(n) = \theta(n) - \theta_r(n). \tag{1}$$

Because angular error compensation at anywhere in the circumference demands the continuous positioning error function, defined as $\varphi(\theta)$, and $\varphi(n)$ is a discrete sequence, it is necessary to obtain $\varphi(\theta)$ with a period of 2π with a fitting algorithm. The harmonic analysis method can meet this requirement.

In the second part of the positioning error compensation, differentiated from previous processing with a computer, we implement the real-time positioning error compensation based on a hardware platform. The hardware platform constantly accepts the value of the turntable angle, θ.

For each value of θ_i, the corresponding positioning error of $\varphi(\theta_i)$ is calculated by the positioning error value calculation unit based on $\varphi(\theta)$. θ_i and $\varphi(\theta_i)$ are transmitted to the positioning error compensation implementation unit simultaneously. Then the compensated turntable positioning angle value is:

$$\theta_{ci} = \theta_i - \varphi(\theta_i). \tag{2}$$

It can be seen that during the dynamic angle measurement, the turntable angle values are put into the hardware platform continuously, and the compensated angle values can be obtained in real time after online calculation and compensation of the positioning error value.

2.2. Principle of harmonic compensation

During real-time positioning error compensation process it is crucial to obtain $\varphi(\theta)$ through $\varphi(n)$. There are various mathematical methods for fitting the positioning error function including harmonic analysis [15], neural network [8], polynomial fitting [14], linear interpolation [10], *etc*. For the characteristics of the periodicity of the turntable positioning error and the superposition of multiple influencing factors, the harmonic analysis is selected to fit the positioning error function.

The ideal positioning error function, $\varphi_0(\theta)$, can be fitted with infinite-order function components:

$$\varphi_0(\theta) = A_0 + \sum_{m=1}^{\infty} C_{\mathrm{m}} \sin(m\theta + \Phi_m), \tag{3}$$

where A_0 is the *direct current* (DC) component, C_m and Φ_m are the amplitude and phase of m-th order component, respectively. C_m and Φ_m can be expressed as:

$$\begin{cases} C_m = \sqrt{A_m^2 + B_m^2} \\ \Phi_m = \tan^{-1} \dfrac{A_m}{B_m} \end{cases}, \tag{4}$$

where and are the coefficients of m-th order harmonic component.

In practice, due to the discrete of the time-domain signal and the negligibility of the high-frequency components, the positioning error function is described as a finite-order compensation form in general as:

$$\varphi(\theta) = A_0 + \sum_{m=1}^{m=M} C_m \sin(m\theta + \Phi_m), \tag{5}$$

where M is the maximum harmonic order of $\varphi(\theta)$, and can be calculated [16] with $\varphi(n)$ as:

$$\begin{cases} A_0 = \dfrac{1}{2N} \displaystyle\sum_{n=1}^{N} \varphi(n) \cos\left[m \cdot \theta_d(n)\right] \\ A_m = \dfrac{2}{N} \displaystyle\sum_{n=1}^{N} \varphi(n) \cos\left[m \cdot \theta_d(n)\right], \quad m = 1, 2, \ldots, \\ B_m = \dfrac{2}{N} \displaystyle\sum_{n=1}^{N} \varphi(n) \sin\left[m \cdot \theta_d(n)\right], \quad m = 1, 2, \ldots \end{cases} \tag{6}$$

where $\theta_d(n)$ are the values around a circle with the equal angle-interval and can be described as:

$$\theta_d(n) = \frac{2\pi n}{N}, \qquad n = 0, 2, \ldots, N. \tag{7}$$

The positioning error function of $\varphi(\theta)$ can be determined combining (4), (5) and (6).

Metrol. Meas. Syst., Vol. 29 (2022), No. 3, pp. 553–571
DOI: 10.24425/mms.2022.142269

3. Analysis of positioning error compensation function

3.1. Surface number of the polygon

We used the harmonic analysis method to fit the continuous positioning error function. The fitting accuracy is directly affected by the maximum harmonic order. Since the period of $\varphi(\theta)$ is 2π, the following relationship holds:

$$\varphi(\theta + 2\pi) = \varphi(\theta). \tag{8}$$

Inverse discrete Fourier transform (IDFT) is then adapted to process (8), and we can get:

$$\sum_{m=0}^{M} F(k_m)\, e^{ikm(\theta \pm 2\pi)} = \sum_{m=0}^{M} F(k_m)\, e^{ikm\theta}, \tag{9}$$

where $e^{ikm\theta}$ and $e^{ikm(\theta \pm 2\pi)}$ are the product vectors in the frequency domain space.

When (9) is satisfied, we obtain the following equation:

$$\begin{cases} e^{\pm ikm2\pi} \equiv 1 \\ k_m = \dfrac{2\pi m}{2\pi} = m, \quad m = 0, 1, ..., M \end{cases}. \tag{10}$$

Based on the symmetry of the *Fourier transform* (FT), only half of the sampling frequency can be intercepted, namely:

$$M = \frac{N}{2}. \tag{11}$$

Since the correspondence of the time domain with the frequency domain, when (11) holds, $\varphi(\theta)$ in (4) can be shown as:

$$\varphi(\theta) = A_0 + \sum_{m=0}^{N/2} C_m \sin(m\theta + \Phi_m). \tag{12}$$

It is known from (3) that $\varphi_0(\theta)$ consists of infinite order harmonic components, but harmonic components that are higher than $N/2$ order cannot be obtained with an N-faced polygon. Therefore, the harmonic components with order greater than $N/2$ will be mixed in ones with order lower than $N/2$, and then the precision of each order component coefficient will be affected.

$$\begin{cases} \Delta A_0 = \displaystyle\sum_{i=1}^{\infty} A_{iN} \\ \Delta A_m = \displaystyle\sum_{i=1}^{\infty} (A_{iN-m} + A_{iN+m}), \quad m = 1, 2, \ldots, \\ \Delta B_m = \displaystyle\sum_{i=1}^{\infty} (B_{iN-m} - B_{iN+m}), \quad m = 1, 2, \ldots \end{cases} \tag{13}$$

where ΔA_0, ΔA_m and ΔB_m are the error values resulting from harmonic mixing for A_0, A_m and B_m respectively.

It can be seen that when N decreases, more high-order components will be mixed in the low-order components. Eventually, the calculated error of C_m and Φ_m increases which leads to the reduction of the accuracy of fitting the positioning error function.

3.2. Calculation parameters of the harmonic function

As shown in Fig. 1, the compensation process of positioning error is performed on the hardware platform, the real-time ability and precision of the method are crucial. The CORDIC algorithm is adapted to resolve the compensation value with $\varphi(\theta)$, and its accuracy is mainly bound by the limited rotational iterations number and the limited data width [17].

3.2.1. Approximate error

The CORDIC algorithm implements the calculation by rotational iterations and approximation of the angle, and the error caused by the limited rotational iterations number, defined as n, is called the angle approximation error. Setting the target angle as γ, the angle approximation error is shown in Fig. 2.

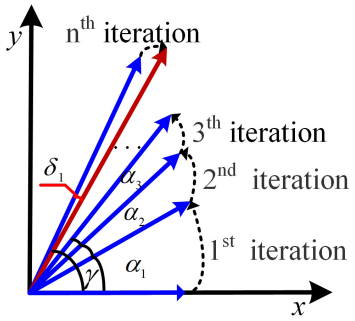

Fig. 2. Schematic diagram of the approximation error.

The rotation angle value of each iterative process of CORDIC is defined as:

$$\alpha_i = \arctan(2^{-i}). \tag{14}$$

The angle value which is obtained by n time iterations is expressed as:

$$\beta = \sum_{i=1}^{n} d_i \cdot \alpha_i \,. \tag{15}$$

In (15), d_i is the rotational direction identifier. When there is clockwise rotation, $d_i = -1$ while $d_i = +1$ when it is counterclockwise. Because n is limited and α_i is fixed, there exists an approximate error, defined as δ_1, which is between the calculated value β after n rotational iterations and the exact angle value γ. It means that γ is in the range of $[\beta - |\delta_1|, \beta + |\delta_1|]$. Since the target angle γ is a random value, δ_1 meets the uniform distribution. The maximum value of the angle approximation error after n rotational iterations can be expressed as:

$$\delta_{1\,\max} = \arctan 2^{-n} < 2^{-n}. \tag{16}$$

As shown in (4), the acquisition of $\varphi(\theta)$ requires the calculation of each order harmonic component which is shown as $\sin(m\theta + \Phi_m)$. The δ_1 affects the calculation accuracy of $\sin(\gamma)$, and introduces the amplitude approximation error which is defined as δ_2 and described as follows:

$$\begin{aligned} \delta_2 &= \sin(\gamma) - \sin(\gamma + \delta_1) \\ &= -2\cos\left(\gamma + \frac{\delta_1}{2}\right)\sin\left(\frac{\delta_1}{2}\right). \end{aligned} \tag{17}$$

Metrol. Meas. Syst., Vol. 29 (2022), No. 3, pp. 553–571
DOI: 10.24425/mms.2022.142269

The maximum value of δ_2 is:

$$|\delta_{2\max}| \leq 2\sin\left(\frac{\delta_{1\max}}{2}\right) < 2^{-n}. \tag{18}$$

It can be seen that the approximation error can be deduced by increasing the value of n, and the larger the value of n, the smaller the value of δ_1 and δ_2.

3.2.2. Rounding error

The calculation process for each order harmonic component of $\varphi(\theta)$ with the CORDIC algorithm not only introduces the approximation error, but also introduces the rounding error due to the limited data width, defined as b.

The i-th rotational iteration process of CORDIC can be expressed by the rotational iteration vector $v(i)$ as follows:

$$v(i+1) = P(i) \cdot v(i), \tag{19}$$

where $P(i)$ is the transformed matrix of the modulus. If we define $Q[*]$ as the rounding operator, subsequently, $Q[v(i)]$ is the vector of $v(i)$ after the rounding and can be described as:

$$Q\left[v(i)\right] = v(i) + e(i), \tag{20}$$

where $e(i)$ is the vector of the rounding error which is introduced by the i-th rotational iteration. The relationship among $v(i)$, $e(i)$ and $Q[v(i)]$ is shown in Fig. 3.

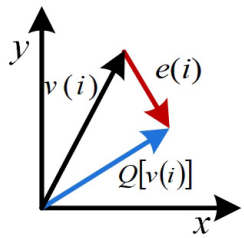

Fig. 3. Schematic diagram of the rounding error.

The vector $e(i)$ is composed of $e_x(i)$ and $e_y(i)$ and the following relationship holds:

$$e(i) \equiv \left[e_x(i),\, e_y(i)\right]. \tag{21}$$

The sizes of $e_x(i)$ and $e_y(i)$ depend on the data width, the maximum rounding error, defined as ε, in the fixed-point calculation is expressed as:

$$\varepsilon = 2^{-b-1}. \tag{22}$$

Therefore, the range of values of (21) is:

$$\begin{cases} |e_x(i) \leq \varepsilon| \\ |e_y(i) \leq \varepsilon| \end{cases}. \tag{23}$$

Combining (22) and (23), the maximum value of the total rounding error introduced by the i-th rotational iteration is:

$$|e(i)| \equiv \sqrt{e_x(i)^2 + e_y(i)^2} \leq \sqrt{2}\varepsilon. \tag{24}$$

The total rounding error in the rotational iterations is composed not only the rounding error introduced by the current rotational iteration but also by the previous ones. Defining as the calculated value after the i-th rotational iteration before rounding, which consists of the true value and the rounding error introduced by previous rotational iterations, gives:

$$Q\left[\hat{v}(i+1)\right] = P(i) \cdot Q\left[\hat{v}(i)\right] + e(i+1). \tag{25}$$

If $e(0) = 0$, the total rounding error vector, defined as $E(n)$, is expressed as follows:

$$E(n) = Q\left[\hat{v}(n)\right] - v(n) = e(n) + \sum_{j=1}^{n-1} \left\{B(j) \cdot e(j)\right\}, \tag{26}$$

where $B(j)$ is the cumulative multiplicative value of $P(i)$. The maximum value of the total rounding error which introduced by n rotational iterations is:

$$\begin{aligned} |E(n)| &\leq |e(n)| + \sum_{j=1}^{n-1} \left| \prod_{i=j}^{n-1} P(i) \cdot e(j) \right| \\ &\leq \sqrt{2}\varepsilon \left\{ 1 + \sum_{j=1}^{n-1} \|B(j)\| \right\} \\ &\leq 2^{-b-0.5} \left\{ 1 + \sum_{j=1}^{n-1} \prod_{i=j}^{n-1} \left(1 + 2^{-2i}\right) \right\}. \end{aligned} \tag{27}$$

From (27), it is known that the $|E(n)|$ is proportional to n and b.

4. Implementation of the real-time compensation method with a harmonic function

As can be seen from Fig. 1, although the positioning error function acquisition is obtained offline, the positioning error compensation should be completed in real-time. Therefore, the hardware platform on which carry out the real-time compensation function should have the characteristics of high processing speed and low system time delay. The flow chart of the positioning error compensation part based on harmonic analysis is shown in Fig. 4.

Positioning error compensation includes three units: an angle value acquisition unit, a positioning error value calculation unit and a positioning error compensation implementation unit. The current value of θ_i is acquired by the angle value acquisition unit and then sent to the positioning error value calculation unit. Based on $\varphi(\theta)$ and θ_i, the compensation value for θ_i, $\varphi(\theta_i)$, is determined by calculation of the phase angle and error component, as well as accumulation of each error component. At last, the compensated turntable positioning angle value, defined as θ_{ci}, is obtained through the subtraction operation of θ_i and $\varphi(\theta_i)$.

During the calculation process of the phase angle and error component, the parallel structure is adapted and the CORDIC algorithm with pipelined structure is used in order to reduce the delay time and ensure the real-time performance of this compensation method.

According to the requirements of the parallel and pipeline structure, an FPGA is selected as the hardware platform. We employed a Cyclone EP4CE115F29C7 from Altera which has the 114480 *logic element* (LE) resources and 3981312 available Memory Bits. The laboratory-made FPGA circuit is shown in Fig. 5.

Metrol. Meas. Syst., Vol. 29 (2022), No. 3, pp. 553–571
DOI: 10.24425/mms.2022.142269

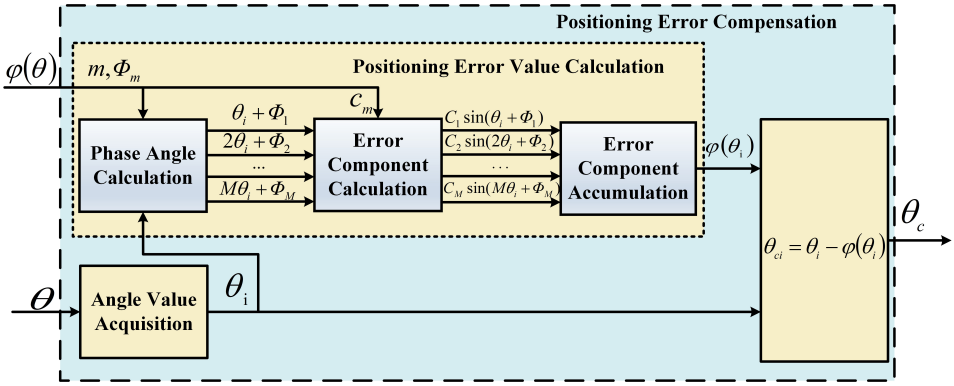

Fig. 4. Diagram of the real-time compensation process.

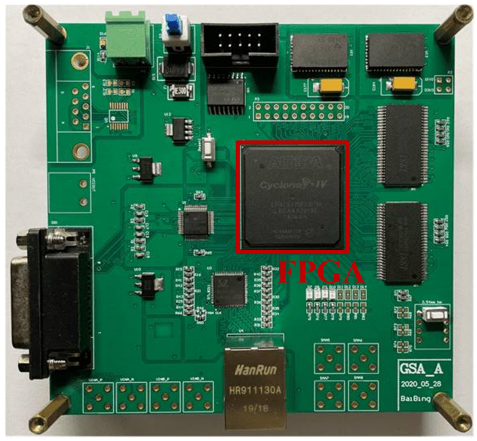

Fig. 5. Laboratory-made electronic board for implementation of real-time compensation.

Since the angle value acquisition is a mature technology, and the positioning error compensation implementation unit and the error component accumulation part, in which there is the positioning error calculation unit, contains only simple adders, only the phase angle calculation part and the error component calculation part are analysed in detail below.

4.1. Calculation of the phase angle

In the phase angle calculation part, the compensation order of m, the *look-up table* (LUT) of Φ_m and the current turntable angle of θ_i are input and the angle of $m\theta_i + \Phi_m$ corresponding to each order harmonic component is output. θ_i is put into the multiplier and the parallel structure is used to output $m-$order angle values of $m\theta_i$ simultaneously. The m is input into LUT and the corresponding angle values of Φ_m to each order harmonic component are output at the same time. When we input $m\theta_i$ and the corresponding Φ_m into m adders respectively, m components of $m\theta_i + \Phi_m$ are obtained simultaneously. The structure is shown in Fig. 6.

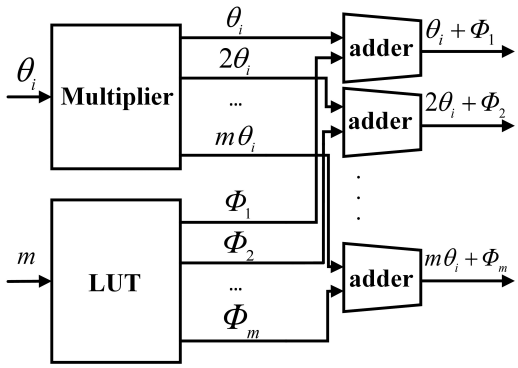

Fig. 6. Schematic diagram of phase angle calculation.

A parallel structure is used in Fig. 6 where m is the compensation order. Since the calculation is performed simultaneously, the increment of m does not increase the system time delay while it increases the complexity of the circuit which leads to the increment of FPGA resource occupation.

The situations with different compensation orders of m are simulated with Quartusii. The resources occupied and the time delay of the phase angle calculation part are shown in Table 1.

Table 1. The effect of compensation order on hardware circuits.

m	2	4	6	8	10	12
LE	16578	22435	27962	36107	43563	49711
Delay cycle	5 cycle	5 cycle	5 cycle	5 cycle	5 cycle	5 cycle
Delay time	100 ns	100 ns	100 ns	100 ns	100 ns	100 ns

As seen in Table 1, as m increases, the LE hardware resources of the FPGA grow, and the occupied LE resource shows an approximately linear relationship with m. When $m = 12$, 43.4% of LE resources are occupied. Because of the parallel structure, the calculation of each order harmonic component is performed simultaneously. m is independent of the time delay which is always 5 cycles. Because the 50 MHz crystal oscillator is used in the laboratory-made FPGA circuit, the time delay **corresponding to** one cycle is 20 ns and 5 cycles mean 100 ns **successively**.

According to (13), the higher the compensation order m is, the higher is the accuracy of the real-time compensation method. Therefore, a larger value of m should be selected, but at the same time the affordability of hardware resources should be considered.

4.2. Calculation of the harmonic component

In the harmonic component calculation part, the CORDIC algorithm is used to obtain $\sin(m\theta_i + \Phi_m)$ which is the compensation function component. C_m is multiplied with $\sin(m\theta_i + \Phi_m)$ through the multiplier to obtain each order harmonic component $C_m \sin(m\theta_i + \Phi_m)$. The pipeline structure which is used in the FPGA for the CORDIC algorithm is shown in Fig. 7.

In Fig. 7, n is the number of rotational iterations. Input angle value $z_0 = m\theta_i + \Phi_m$, which is equivalent to γ in Fig. 2, and its corresponding x_0 and y_0 for rotational iterations are subjected to crossover operations. The x_i and y_i are processed to obtain y_{i+1} and x_{i+1} respectively. z_i is rotated

Metrol. Meas. Syst., Vol. 29 (2022), No. 3, pp. 553–571
DOI: 10.24425/mms.2022.142269

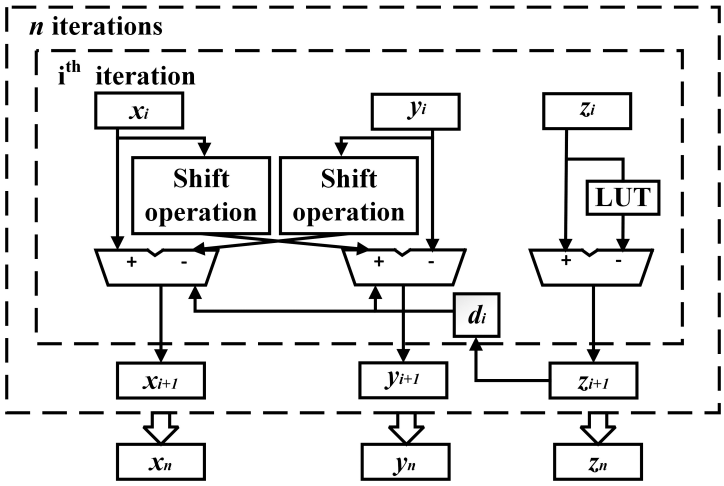

Fig. 7. Pipeline structure of the CORDIC algorithm.

to get z_{i+1} and the sign judgment signal, which d_i is used to determine the positive and negative in the x_i and y_i operations. After $n$time iterations, the final output value is $y_n = \sin(m\theta_i + \Phi_m)$, where z_n approaches to zero.

Variations in n and b have an impact on the hardware resource occupied and the extent of system latency. In this paper, we use a 24-sided polygon, so M is limited to 12 based on (11). m is set equal to 12 and the values of n and b are selected accordingly. The analysis results with using Quartusii are shown in Table 2.

Table 2. Effect of n and b on hardware circuits.

n	15		16	
b	30	32	30	32
LE	45648	47602	47594	49711
Delay cycle	15 cycle	15 cycle	16 cycle	16 cycle
Delay time	300 ns	300 ns	320 ns	320 ns

As can be seen from Table 2, the increment of the bit width will increase the LE resource occupation, but will not increase the system latency. The extent of system latency in this part is only related to the rotational iterations number. The bigger is the n, the larger is the system latency.

Moreover, an increment of n and b can reduce the arithmetic error while it increases the complexity of the hardware circuit and the amount of resources occupied. The error which is generated during the compensationof the positioning error should be less than the angle resolution of the circumferential goniometric system which is defined as R and can be described as

$$R = \frac{360}{s \cdot l}, \tag{28}$$

where l is the number of circumferential lines on the grating code disk; s is the periodic subdivision number in one grating pitch. In this paper, $l = 16384$ and $s = 1024$, so the upper limit of the

approximation error is

$$\arctan(2^{-n}) < R = 2.146 \times 10^{-5}. \tag{29}$$

From (29), it is known that $n = 16$ satisfies the required accuracy, and according to (27) and the required accuracy, $b = 30$ and 32 can satisfy the accuracy requirements. The delay time of each part in this case is shown in Table 3.

Table 3. Time delay for each hardware compensation unit.

Compensation unit	Angle value acquisition	Positioning error value calculation	Positioning error compensation implementation
Delay cycle	9 cycle	25 cycle	4 cycle
Delay time	180 ns	500 ns	80 ns

It is known from Table 3 that the compensation method on the FPGA platform requires a 38 cycle delay. Because the time delay of 1 cycle is 20 ns, the time delay of 38 cycles corresponds to 760 ns which means that the proposed compensation method has a high real-time characteristic.

5. Experiment and data analysis

The effectiveness of the continuous positioning error function which is fitted with the harmonic analysis method should be proved first. The linear interpolation method, the polynomial method and the harmonic analysis method are used to fit the continuous positioning error function respectively and the compensation results are compared. Then, the effects of parameters of m, n and b on the accuracy of $\varphi(\theta)$ are tested. Finally, the real-time compensation process with $\varphi(\theta)$ is performed on a turntable, and the effectiveness and feasibility of the compensation method we proposed is verified.

In this paper, the positioning error sequence of a turntable of $\varphi(n)$ is obtained by using the combination of an autocollimator and a 24 faced-polygon. The calibration process is shown in Fig. 8.

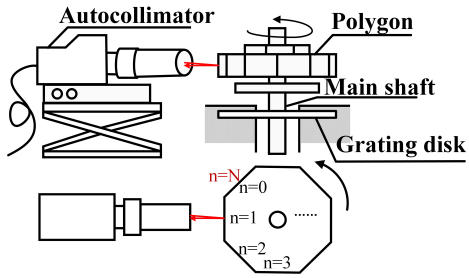

Fig. 8. Schematic diagram of the calibration process.

In the first step of the calibration process, the turntable is rotated to make one of the surfaces of the polygon, which is coaxial with the grating disk, aligned with the autocollimator ($n = 0$). On this condition, the angular position is regarded as relative zero and the positioning error which is measured by the autocollimator is recorded as $\varphi(0)$. Then, the turntable is rotated for the angle of $2\pi/N$ to make the next working face of the polygon aligned with the autocollimator.

Metrol. Meas. Syst., Vol. 29 (2022), No. 3, pp. 553–571
DOI: 10.24425/mms.2022.142269

The positioning error is $\varphi(1)$. After n time rotations, the turntable returns to the relative zero position and the positioning error value sequences of each position, recorded as $\varphi(n)$ $(n = 0 \ldots N)$, are obtained.

In this calibration process, the high-precision instruments are the guarantee of the accuracy of obtained $\varphi(n)$. Table 4 lists the specifications of the main instruments and devices used in the experiment.

Table 4. Specifications of main instruments and devices.

Instrument name	Model	Precision
Autocollimator	ELCOMAT3000	$-1000'' \sim +1000''$ $Ui = 0.25''$
Polygon	24-sided polygon	$\pm 1''$
Grating disk	R10851(MicroE)	16384 inscribed lines Grid pitch: 20 μm
Reading head	Mercury's sensor	Rotary: up to $\pm 2.1''$
Turntable	High precision air flotation turntable	Repeatability: $0.3''$ Accuracy: $\pm 0.5''$

5.1. Validation of the harmonic compensation method

The 24-faced polygon is adapted in Fig. 8 to obtain the positioning error sequence of $\varphi(n)$. To prove the validation of harmonic compensation, the linear interpolation method [10] and the polynomial method [14] are used to construct compensation functions separately and then the compensation results are compared with the harmonic analysis compensation method.

In the experiment, the odd-number-faced data of $\varphi(n)$ are selected as the original data to establish $\varphi(\theta)$ with the linear interpolation method, the polynomial method and the harmonic analysis method, respectively while the even-number-faced data of $\varphi(n)$ are selected as the reference values to verify the effect of methods. The value of $\varphi(\theta)$ fitted with the three methods are sampled at even-number-faced angle positions and then subtracted from the corresponding value of $\varphi(n)$, respectively. The results of the experiment are shown in Fig. 9.

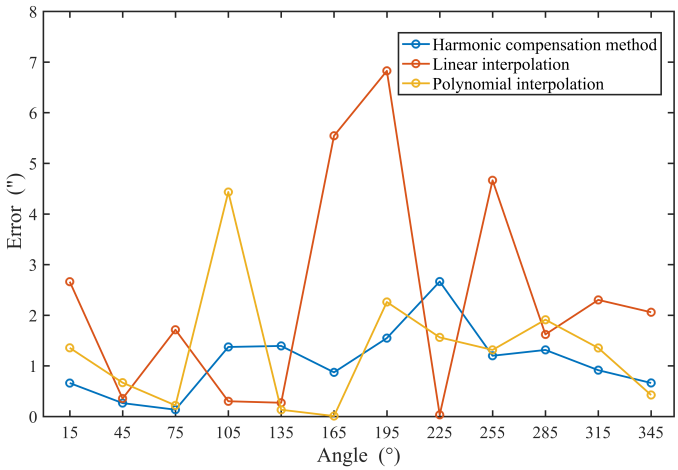

Fig. 9. Comparison of compensation results of the three fitting methods.

It can be seen from Fig. 9 that the compensation precision of linear interpolation and the polynomial method are fluctuated greatly due to the small number of calibration points within the circumference, with maximum errors of 6.83″ and 4.43″ and the average errors of 2.36″ and 1.30″, respectively. The $\varphi(\theta)$ constructed by the harmonic analysis method matches the positioning error of the turntable in principle, and achieves a higher precision with the maximum error of 2.67″ and an average error of 1.08″.

5.2. Effects of parameters

The $\varphi(n)$ which is obtained from the 24-faced polygon is used to construct the corresponding $\varphi(\theta)$. The effects of m, n and b on the error introduction of the compensation process are analysed with MATLAB.

The $\varphi(\theta)$ with different values of m are sampled at $\theta_d(n)$ and compared with $\varphi(n)$ which is obtained by calibration. The results are shown in Fig. 10.

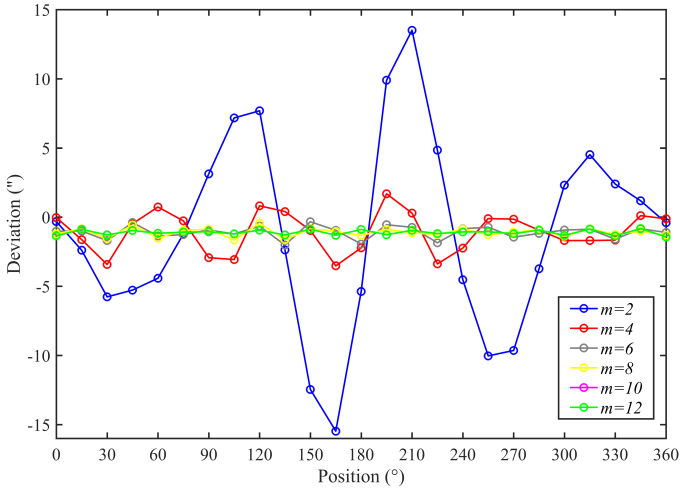

Fig. 10. Influence of m on compensation accuracy.

It can be seen in Fig. 10 that the higher $m$is, the closer $\varphi(\theta)$ and $\varphi(n)$ are and the smaller the range of the error curve is. The accuracy of $\varphi(\theta)$ improves slowly with increasing m. When $m \geq 6$, the fitting error of $\varphi(\theta)$ fluctuates in the range of $[-2.02'', -0.34'']$ while when $m \geq 10$, the error does not decrease significantly with the increase of m.

The accuracy of $\varphi(\theta)$ is also related to the iteration number and bit width. The effects of n and b on the approximation error and rounding error are analysed using MATLAB, and the results are shown in Fig. 11.

Fig. 11a shows the effect of n and b on the rounding error. The rounding error decreases with the increasing b and then improves the accuracy of $\varphi(\theta)$. When $b < 26$, the rounding error increases with the increment of iteration number n and when $b \geq 26$ bits, the rounding error is approximately equal for different n.

Fig. 11b shows the effect of n on the approximation error. With the increment of n, the approximation error converges rapidly, and shrinks by approximately half with each 1 added to n of the process.

Metrol. Meas. Syst., Vol. 29 (2022), No. 3, pp. 553–571
DOI: 10.24425/mms.2022.142269

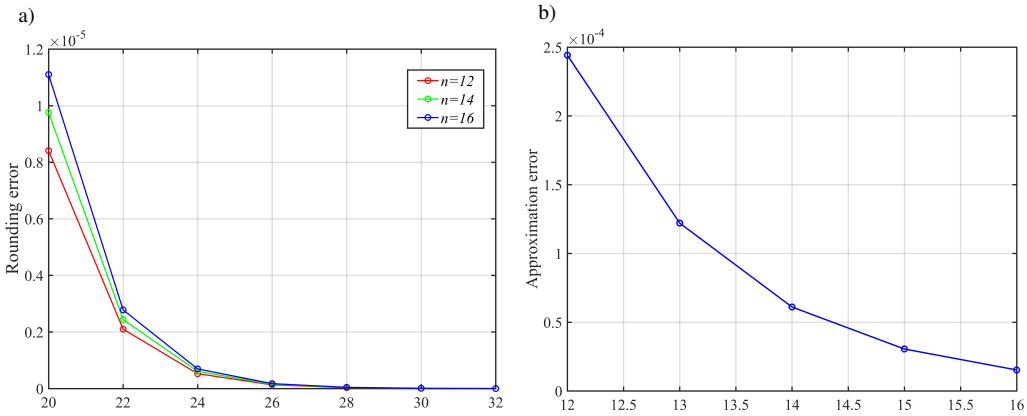

Fig. 11. Schematic diagram of the approximation error and the rounding error.

Comparing the magnitudes of the two types of errors, we can conclude that the approximation error has a greater impact on the accuracy of $\varphi(\theta)$. So, increasing the rotational iterations number should be considered the first way to improve the accuracy of $\varphi(\theta)$.

5.3. Reliability analysis of harmonic compensation

In order to continue the verification of e effectiveness of the harmonic compensation function for application in the turntable goniometric systems, we built a test platform based on the calibration setup shown in Fig. 8 with a laboratory-made FPGA circuit to evaluate the effect of real-time compensation with $\varphi(\theta)$. We use the calibration setup to obtain the corresponding $\varphi(n)$ and construct $\varphi(\theta)$ with the harmonic analysis method. Combined with Fig. 10 and Fig. 11, $m = 10$, $n = 16$, and $b = 32$ are chosen for the test; the real-time compensation using the harmonic function is performed on the laboratory-made circuit board which output the compensated angle value θ_c directly. The test platform is shown in Fig. 12.

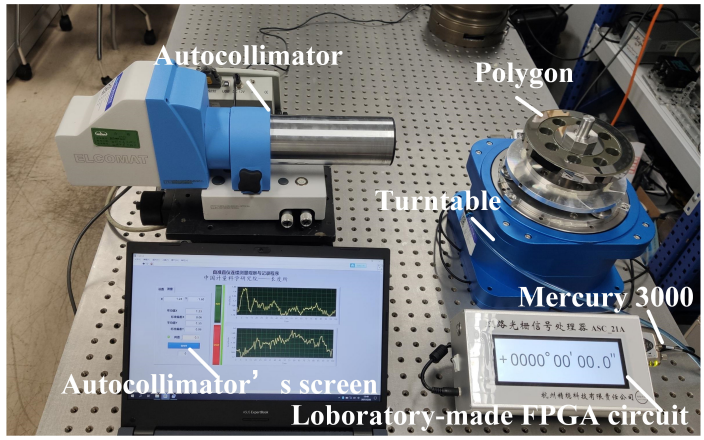

Fig. 12. Photograph of the test platform.

Due to the parallel structure adapted in Fig. 6, the change of compensation order of $\varphi(\theta)$ does not affect the amount of time delay. The time delay of the positioning error compensation process in the test platform presented in Fig. 12 is 38 cycles or 760 ns. It shows that the method has high real-time characteristics.

The compensated positioning error of the turntable, defined as $e(\theta_i)$, is obtained through the calibration setup with the **autocollimator and the polygon, shown as Fig. 8, and the continuous positioning error function $\varphi(\theta)$ is calculated with the harmonic analysis algorithm, shown as Formula (12). The compensation function of $\varphi(\theta)$ is downloaded to the laboratory-made FPGA circuit, shown in Fig. 5, and used to compensate the positioning error in real-time.** The results are shown in Fig. 13.

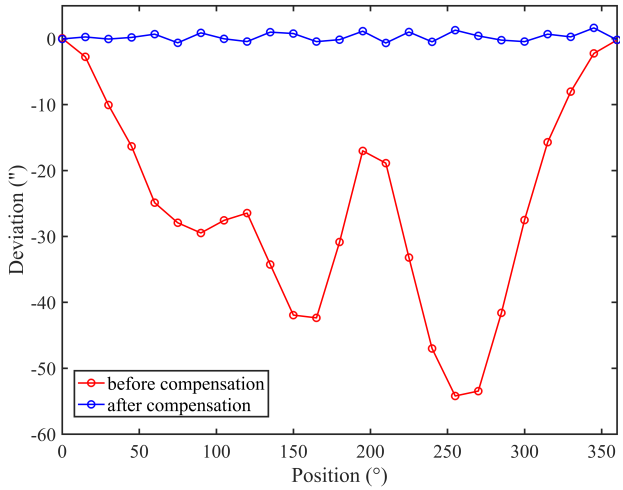

Fig. 13. Comparison of the positioning error before and after compensation.

After being compensated with 10^{th} order harmonic function, the positioning error fluctuates within $[-0.66'', 1.63'']$ and the maximum positioning error is reduced from $54.21''$ to $1.63''$. That means the effect of reducing 96.99% of the positioning error has been achieved.

Fourier spectrum analysis was performed on the positioning errors shown in Fig. 13; the results of the analysis are shown in Fig. 14.

It can be seen from Fig. 14 that in the error function before compensation, the higher is the order of the harmonic component, the smaller is the amplitude. It is in line with the amplitude distribution of the turntable positioning error.

In the error function after compensation, comparing with the original one, all of the amplitudes of components of the first 10 orders have been reduced after compensation, especially those of the first 4 orders. Since the corresponding error sources for the first 4 orders are relatively single, more than 95% of the positioning error of those can be reduced by compensation. Meanwhile, about 76% of the positioning error of first 6 orders can be suppressed with harmonic function compensation.

Combined with Fig. 11 and Fig. 14, it can be seen that to further improve the positioning precision of the turntable, it is preferred to consider increasing the number of iterations. Secondly, the method of increasing the order of $\varphi(\theta)$ can be considered. Since the rounding error is smaller than the approximation error, the amount of error that can be reduced by increasing the b is small when $b \geq 26$.

Metrol. Meas. Syst., Vol. 29 (2022), No. 3, pp. 553–571
DOI: 10.24425/mms.2022.142269

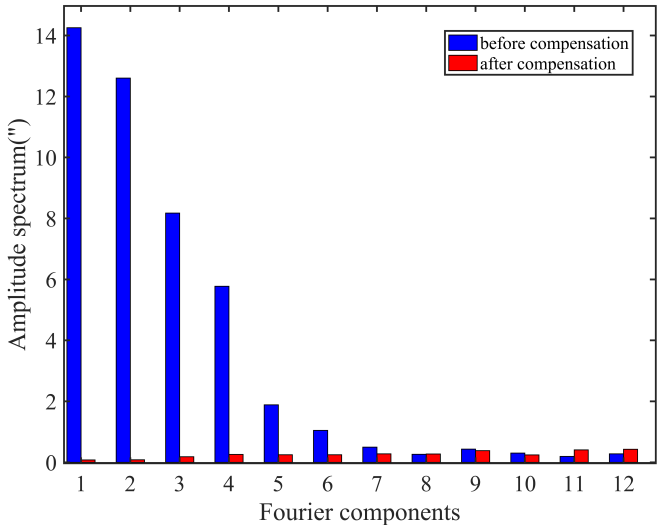

Fig. 14. Results of spectrum analysis of positioning errors.

6. Conclusions

For improving the positioning precision of the turntable, a real-time compensation method with harmonic analysis was proposed.

First, we studied the principle of real-time compensation and the harmonic analysis. Then, the surface number of the polygon, number of rotational iterations and data width were analysed and the corresponding quantitative error models of harmonic function error, rounding error and approximation error were established, separately. Next, we proposed a hardware construct for the positioning error real-time compensation method, and analysed the resource consumption and system latency of the phase angle calculation part and the harmonic component calculation part in relation to the key parameters m, n and b. This method occupies 43.4% LE resources of the FPGA, and diminishes the system latency to less than 760 ns. Comparing with other mainstream software compensation methods which use a host computer to compensate the positioning error off-line, this method has a better real-time performance. Finally, experiments were performed with a test platform with a laboratory-made FPGA circuit to verify the real-time performance, feasibility and effectiveness of the harmonic positioning error compensation method. The effectiveness of the compensation method is verified by comparing the compensation effects of the linear interpolation and polynomial methods. The harmonic analysis method we proposed has the best effect: maximum error of 2.67″, and the average error of 1.08”.

The results proved with the harmonic compensation method proposed in this paper improved the positioning precision of the turntable from 54.21″ to 1.63″, equivalent to 96.99% reduction in the positioning error.

Acknowledgements

This research was financially supported by the National Natural Science Foundation of China (52175526), the project of the National Key R&D Program of China (2017YFF0204901), and the research project of General Administration of Quality Supervision, Inspection and Quarantine of PRC (2016QK189).

References

[1] Just, A., Krause, M., Probst, R., Bosse, H., Haunerdinger, H., Spaeth, Ch., Metz, G., & Israel, W. (2009). Comparison of angle standards with the aid of a high-resolution angle encoder. *Precision Engineering*, *33*(4), 530–533. https://doi.org/10.1016/j.precisioneng.2009.02.004

[2] Probst, R., Wittekopf, R., Krause, M., Dangschat, H., & Ernst, A. (1998). The new PTB angle comparator. *Measurement Science and Technology*, *9*(7), 1059–1066. http://dx.doi.org/10.1088/0957-0233/9/7/009

[3] Watanabe, T., Fujimoto, H., Nakayama, K., Masuda, T., & Kajitani, M. (2001). Automatic high-precision calibration system for angle encoder. *Lasers in Metrology and Art Conservation*, Germany, 267–274. https://doi.org/10.1117/12.445630

[4] Watanabe, T., Fujimoto, H., Nakayama, K., Masuda, T., & Kajitani, M. (2003). Automatic high-precision calibration system for angle encoder (II). *Optical Science and Technology, SPIE's 48th Annual Meeting*, United States, 400–409. https://doi.org/10.1117/12.506473

[5] Watanabe, T., Kon, M., Nabeshima, N., & Taniguchi, K. (2014). An angle encoder for super-high resolution and super-high accuracy using SelfA. *Measurement Science and Technology*, *25*(6):065002. http://dx.doi.org/10.1088/0957-0233/25/6/065002

[6] Huang, Y., Xue, Z., Huang, M., & Qiao, D. (2018). The NIM continuous full circle angle standard. *Measurement Science and Technology*, *29*(7), 074013. https://doi.org/10.1088/1361-6501/aac6a6

[7] van Eekeren, A. W., Schutte, K., Dijk, J., Schwering, P. B., van Iersel, M., & Doelman, N. J. (2012). Turbulence compensation: an overview. *SPIE Defense, Security, and Sensing*, United States, 83550Q. https://doi.org/10.1117/12.918544

[8] Dhar, V., Tickoo, A., Kaul, S., Koul, R., & Dubey, B. (2009). Artificial neural network-based error compensation procedure for low-cost encoders. *Measurement Science and Technology*, *21*(1), 015112. https://doi.org/10.1088/0957-0233/21/1/015112

[9] Gao, G. B., Wang, W., Xie, L., Wei, D. B., & Xu, W. Q. (2011). Study on the compensation for mounting eccentric errors of circular grating angle sensors. *Advanced Materials Research*, *301-303*, 1552–1555. https://doi.org/10.4028/www.scientific.net/AMR.301-303.1552

[10] Lopez, J., & Artes, M. (2012). A new methodology for vibration error compensation of optical encoders. *Sensors*, *12*(4), 4918–4933. https://doi.org/10.3390/s120404918

[11] Yu, Y., Dai, L., Chen, M. S., Kong, L. B., Wang, C. Q., & Xue, Z. P. (2020). Calibration, Compensation and Accuracy Analysis of Circular Grating Used in Single Gimbal Control Moment Gyroscope. *Sensors*, *20*(5), 1458. https://doi.org/10.3390/s20051458

[12] Jia, H. K., Yu, L.D., Jiang, Y. Z., Zhao, H. N. & Cao, J. M. (2020). Compensation of rotary encoders using Fourier expansion-back propagation neural network optimized by genetic algorithm. *Sensors*, *20*(9), 2603. https://doi.org/10.3390/s20092603

[13] Du, Y. B., Yuan, F., Jiang, Z. Z., Li, K., Yang, S. W., Zhang, Q. B., Zhang, Y. H., Zhao, H. L., Li, Z. R. & Wang, S. L. (2021). Strategy to Decrease the Angle Measurement Error Introduced by the Use of Circular Grating in Dynamic Torque Calibration. *Sensors*, *21*(22), 7599. https://doi.org/10.3390/s21227599

[14] Gurauskis, D., Kilikevičius, A. & Kasparaitis, A.(2021). Thermal and Geometric Error Compensation Approach for an Optical Linear Encoder. *Sensors*, *21*(2), 360. https://doi.org/10.3390/s21020360

[15] Hu, Y., Zhan, Y., Han, L., Hu, P., Ye, B. & Yu, Y. (2020). An Angle Error Compensation Method Based on Harmonic Analysis for Integrated Joint Modules. *Sensors*, *20*(6), 1715. https://doi.org/10.3390/s20061715

Metrol. Meas. Syst., Vol. 29 (2022), No. 3, pp. 553–571
DOI: 10.24425/mms.2022.142269

[16] Zhang, G., Zhang, X. F., Wang, W. F., Cao, Y. M., & Zhao, J. (2016). Study on error compensation of angular position measurement. *Journal of Test and Measurement Technology*, *30*(4), 353–357. https://doi.org/10.3969/j.issn.1671-7449.2016.04.012

[17] Hu, Y. H. (1992). The quantization effects of the CORDIC algorithm. *IEEE Transactions on Signal Processing*, *40*(4), 834–44. https://doi.org/10.1109/78.127956

Yi Zhou received her B.Sc. degree from China Jiliang University in 2020. She is currently pursuing her master degree at China Jiliang University. Her research interest is the turntable positioning compensation.

Weibin Zhu (Corresponding author) received his Ph.D. degree in control theory and control engineering from Zhejiang University in 2014. He is currently an associate professor at China Jiliang University. His current interests include the grating signal processing and precision angle measurement.

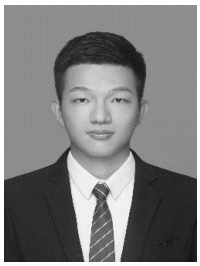

Yi Shu received his B.Sc. degree from Jiangxi University of Science and Technology in 2019. He is currently pursuing his M.Sc. degree at China Jiliang University. His research interest is turntable positioning compensation.

Wei Zou received his Ph.D. degree from the School of Instrumentation and Optoelectronic Engineering of Beihang University in 2020. He is currently working on a postdoctoral position in the Institute of Geometric Metrology, Chinese National Institute of Metrology. His research interests include geometric metrology and computer vision problems related to high accuracy camera calibration as well as three-dimensional reconstruction with multi-cameras.

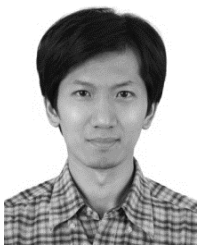

Yao Huang received his B.Sc. degree and M.Sc. degree both from Beijing University of Technology in 2004 and 2007, respectively. He worked at the Geometric Lab of Beijing Metrology Institute from 2007 to 2013 and joined the Division of Metrology in Length and Precision Engineering of National Institute of Metrology in 2013. He is currently pursuing his Ph.D. degree at Zhejiang University. His main research interest is angle measurement..

Zi Xue received her Ph.D. degree from Harbin Technical University in 2006. She joined the Division of Metrology in Length and Precision Engineering of the National Institute of Metrology in 1991. She is currently the chairman of the Technical Committee of Length (TCL) of the Asia Pacific Metrology Programme (APMP), the member of Consultative Committee for Length (CCL) of the International Committee for Weights and Measures (CIPM). Her main research interest is geometric measurement.